Regulatory effects of miRNA-181a on FasL expression in bone marrow mesenchymal stem cells and its effect on CD_4^+T lymphocyte apoptosis in estrogen deficiency-induced osteoporosis

BINGYI SHAO[1-3], XIAOHUI FU[4], YANG YU[1-3] and DEQIN YANG[1-3]

[1]Department of Operative Dentistry and Endodontics, Affiliated Hospital of Stomatology; [2]Chongqing Key Laboratory of Oral Diseases and Biomedical Sciences, Affiliated Hospital of Stomatology; [3]Chongqing Municipal Key Laboratory of Oral Biomedical Engineering of Higher Education, Affiliated Hospital of Stomatology, Chongqing Medical University, Chongqing 401147; [4]Department of Orthodontics, Second Affiliated Hospital, College of Medicine, Zhejiang University, Hangzhou, Zhejiang 310003, P.R. China

Received July 28, 2017; Accepted April 19, 2018

DOI: 10.3892/mmr.2018.9026

Abstract. Post-menopausal osteoporosis is a bone formation disorder induced by estrogen deficiency. Estrogen deficiency facilitates the differentiation and maturation of osteoclasts by activating T lymphocytes. In our previous study, it was demonstrated that estrogen promotes bone marrow mesenchymal stem cell (BMMSC)-induced osteoclast apoptosis through down-regulation of microRNA (miR)-181a and subsequent Fas ligand (FasL) protein accumulation. In the present study, the regulatory effects of miR-181a on FasL expression in BMMSCs and the apoptotic effects of BMMSCs on cluster of differentiation $(CD)_4^+$T lymphocytes were investigated. An ovariectomized mouse model of osteoporosis (OVX) was established and CD4$^+$T lymphocytes were isolated from the bones of these mice. The results demonstrated that the number of CD4$^+$T lymphocytes was increased in the OVX group compared within the control group, thus suggesting that estrogen deficiency may increase CD4$^+$T lymphocyte number. CD4$^+$T lymphocytes were subsequently co-cultured with estrogen-treated BMMSCs, after which it was demonstrated that estrogen significantly promoted the apoptosis of CD4$^+$T lymphocytes. Western blot analysis indicated that estrogen promoted the apoptosis of CD4$^+$T lymphocytes through regulation of FasL expression in BMMSCs in a concentration-dependent manner. Finally, miR-181a was transfected into BMMSCs, which were co-cultured with CD4$^+$T lymphocytes *in vitro* and *in vivo*. The results revealed that miR-181a exerted a negative regulatory effect on BMMSC-induced CD4$^+$T lymphocyte apoptosis by regulating FasL protein expression in BMMSCs; this maybe a key mechanism underlying the development of estrogen deficiency-induced osteoporosis.

Correspondence to: Mrs. Deqin Yang, Department of Operative Dentistry and Endodontics, Affiliated Hospital of Stomatology, Chongqing Medical University, 426, North Songshi Road, Yubei, Chongqing 401147, P.R. China
E-mail: yangdeqincq@126.com

Abbreviations: BMMSCs, bone marrow mesenchymal stem cells; FasL, Fas ligand; PMO, post-menopausal osteoporosis

Key words: bone marrow mesenchymal stem cells, estrogen, FasL, microRNA-181a, osteoporosis

Introduction

Post-menopausal osteoporosis (PMO) is one of the most common types of osteoporosis. In 2008, the number of patients with PMO in China was estimated to be 100 million. The key symptoms of PMO include sex hormone disorder and immune imbalance, which leads to an imbalance between bone formation and bone resorption, where bone formation is significantly weakened (1). Clinical manifestations of PMO include a decrease in bone mass and deterioration of the bone microstructure, as well as an increase in bone brittleness, resulting in a higher fracture risk. The pathogenesis of PMO is well established; the disease is induced by estrogen deficiency as a result of ovarian function failure in post-menopausal women (2).

The regulatory effects of estrogen on bone metabolism occur through numerous mechanisms. For example, estrogen mediates the balance of bone resorption and bone formation by regulating parathyroid hormone. In addition, estrogen integrates with osteoblast receptors to promote bone formation. There are several growth factors involved in the regulatory effects of estrogen on bone metabolism, including interleukin (IL)-1, IL-6, IL-7, tumor necrosis factor (TNF)-α, transforming growth factor-β and interferon (IFN)-γ (3-6). Estrogen deficiency may directly or indirectly increase the number of B lymphocytes by increasing the expression levels of IL-7, of which promotes the expression of proinflammatory cytokines by T lymphocytes and macrophages, leading to bone mass loss (7,8). The inflammatory cytokines expressed by CD4$^+$T lymphocytes have the most significant effects on bone cell function. CD4$^+$T lymphocytes are divided into four

main subpopulations: T helper (Th)1, Th2, Th17 cells promote osteoclast growth via the expression of receptor IFN-γ, IL-6, and IL-17 respectively (9). Among these four osteoclastogenic cytokines, RankL has a particularly important role in bone resorption: *In vitro* co-culture of murine bone marrow-derived pre-osteoclasts with $CD4^+$T lymphocytes leads to osteoclast differentiation and maturation (10). Emerging evidence has indicated an important role for estrogen in balancing osteoblasts and osteoclasts, through regulation of Fas/Fas ligand (FasL) signaling pathways. Fas is activated in response to FasL integration with the surface of cells expressing Fas. The activated Fas subsequently results in accumulation of adaptin in the cytoplasm by interaction of its intracellular death domain (DD) with the carboxyl terminal DD of the Fas-associated protein with death domain (FADD). The accumulated FADD integrates with caspase-8 through its death effect domain to form the death-inducing signaling complex, which activates the downstream caspase family and cell apoptosis (11,12). It has been revealed that estrogen can regulate the expression of FasL on the surface of osteoblasts and osteoclasts, causing osteoclast apoptosis by disrupting the bone dynamic balance (13,14).

Bone marrow mesenchymal stem cells (BMMSCs) are osteoblast precursor cells. It has been demonstrated that BMMSCs exert regulatory effects on immunocytes (10). BMMSCs may inhibit the growth of T lymphocytes at the G_0/G_1 stage of the cell cycle and suppress T lymphocyte proliferation (15,16). Furthermore, BMMSCs reduce the release of IFN-γ by activated T lymphocytes, and inhibit the proliferation and differentiation of B lymphocytes, natural killer cells and neutrophils (17). Previous research has indicated that BMMSCs have the ability to generate a variety of terminally differentiated mesenchymal cells, such as osteoblasts and chondrocytes, which are key in bone construction (18).

MicroRNAs (miRNAs/miRs) have several target genes and extensively participate in the gene regulatory network to exert various biological effects. Research suggests that miRNAs are key regulatory factors of the downstream network, to a greater extent than other regulatory factors and/or ligands (19). Previous work has indicated that miRNAs are key in the regulation of bone functional cell apoptosis. For example, miR-21 regulates expression of the FasL gene; therefore, the apoptotic rate of osteoclasts transfected with miR-21 is reduced, leading to the development of osteoporosis (20).

Our previous study demonstrated that BMMSCs induce osteoclast apoptosis *in vitro* and *in vivo*, and the addition of estrogen promotes BMMSCs-induced osteoclast apoptosis by increasing FasL protein expression. Further investigation revealed that estrogen maintains FasL protein accumulation by downregulating miR-181a expression (21). In the present study, $CD4^+$T lymphocytes were selected as a cell model to elucidate the regulatory effects of the signaling molecules involved in the development of estrogen deficiency-induced osteoporosis. Ovariectomized mice were used as a model of osteoporosis, and BMMSCs and $CD4^+$ T lymphocytes were subsequently isolated from osteoporotic and control mice. The apoptotic effect of BMMSCs isolated from the different groups on $CD4^+$ T lymphocytes was evaluated, and the effects of estrogen on BMMSCs-induced $CD4^+$ T lymphocyte apoptosis were investigated. Subsequently, the regulatory effects of estrogen on FasL expression in BMMSCs were evaluated. BMMSCs were transfected with miR-181a and co-cultured with $CD4^+$T lymphocytes, both *in vitro* and *in vivo*, to reveal the regulatory effect of miR-181a on FasL protein expression in BMMSCs and the effects of miR-181aon $CD4^+$T lymphocyte apoptosis.

Materials and methods

Materials. α-Minimum Essential Media (MEM), RPMI-1640 and trypsin were purchased from Gibco (Thermo Fisher Scientific, Inc., Waltham, MA, USA). Goat anti-mouse CD45 (cat. no. ab65952), CD105 (cat. no. ab2529), stem cell antigen-1 (Sca-1; cat. no. ab25323) and CD29 (cat. no. ab17981) monoclonal antibodies were purchased from Abcam (Cambridge, MA, USA) and used for testing mesenchymal stem cells surface markers. CD3 (cat. no. 100243) and CD28 (cat. no. 102109) antibodies were purchased from BioLegend, Inc. (San Diego, CA, USA) and used for activation of T lymphocytes. Rabbit anti-mouse FasL (cat. no. sc-19988) and β-actin (cat. no. sc-69879) antibodies from Santa Cruz Biotechnology, Inc. (Dallas, TX, USA) for FasL expression detection and normalization. Reagents for the induction of BMMSC differentiation, including dexamethasone, vitamin C, phosphate, β-phosphoglycerol, 3-isobutyl-1-methylxanthine (IBMX), insulin and transferrin were purchased from Sigma-Aldrich (Merck KGaA, Darmstadt, Germany). TRIzol reagent, Lipofectamine® 2000 transfection reagent, miR-181a mimics, miR-181a inhibitor and miR-181a control were purchased from Invitrogen (Thermo Fisher Scientific, Inc.). GoldView™ nucleic acid gel stain (cat. no. 10201ES03) was purchased from Beijing SBSGenetech Co., Ltd. (Beijing, China). SYBR Green I *Premix ExTaq*™ (Cat. RR42LR), λ DNA-HindIII digest (cat. no. 3403), 50 bp DNA ladder (cat. no. 3421A), DL2000 DNA marker (cat. no. 3427A) and the miRNA assay kit (cat. no. 631435) were purchased from Takara Biotechnology Co., Ltd. (Dalian, China).

Mice osteoporosis model. All the experiments were performed on a total of 40 8-week-old female C57 mice (22-25 g), which were obtained from the Laboratory Animal Center of the Fourth Military Medical University (Xi'an, China).Bilateral ovaries were resected to establish the osteoporosis model within 20 mice (OVX group). The control group (n=20) were subjected to a similar surgery, with the exception that instead of ovary removal, a small amount of adipose tissue was removed (sham group). All mice were housed in a specific pathogen-free (SPF) environment (22˚C, 12 h light/dark cycle, and 50-55% humidity) with free access to food and water. The present study was approved by the ethics committee of Chongqing Medical University (Chongqing, China).

Microtomography (Micro-CT). After 2 months maintenance in a SPF room, mice in the OVX and sham groups, or mimic BMMSCs, inhibitor BMMSCs and control BMMSCs groups were anaesthetized by intraperitoneal injection of pentobarbital sodium and placed on Micro-CT apparatus for an intravital scan of the proximal femoral area. The micro-CT scan was performed using a scanning angle of 360˚ and a resolution of 9 μm along the long axis of the femur. Following the Micro-CT scan, an area of 1 mm below the growth plate

and 1.5 mm from the distal femur was selected as the range of interest and a three-dimensional image of the trabecular bone was reconstructed. Finally, parameters representing the spatial structure of trabecular bone, including bone volume relative to tissue volume (BV/TV;%), trabecular thickness (Tb.Th; μm), trabecular spacing (Tb.Sp; mm) and trabecula number (Tb.N; 1/mm) were analyzed and determined using the built-in software (Inveon Research Workplace 2.2, Siemens Healthineers, Erlangen, Germany).

Isolation of CD4$^+$T lymphocytes. After 2 months maintenance in a SPF room, mice in the OVX and sham groups were anaesthetized with 100 mg/kg pentobarbital sodium, decapitated and immersed in 75% alcohol with a temperature of 4˚C for 5 min. The left abdomen skin of the mice was cut, and the subcutaneous tissue and abdominal muscles were separated to expose the spleen. Spleens were collected and peripheral connective tissues were removed, after which spleens were placed in PBS. Subsequently, the obtained spleens were minced and squeezed using tweezers under sterile conditions, in order to obtain a cell suspension. The cell suspension was transferred into sterile tubes and centrifuged at 400 x g for 3 min at 4˚C. The supernatant was removed prior to the addition of 2 ml 1X Red Blood Cell Lysis Buffer (Beyotime Institute of Biotechnology, Haimen, China) at 4˚C for 5 min for complete red blood cell lysis. The cell suspension was centrifuged again at 400 x g for 3 min in 4˚C after which the supernatant was removed, and pellets were collected and washed twice with PBS. CD4 antibody (cat. no. 100413, purity ≥95% high-performance liquid chromatography; BioLegend, Inc.) was used for isolation of CD4$^+$ lymphocytes. Monocytes were stained with fluorescent CD4$^+$ antibody for 30 min at room temperature and without light. Finally, CD_4^+T lymphocytes were obtained. To determine the concentration of CD_4^+T lymphocytes, CD4$^+$T lymphocytes were fixed with 4% paraformaldehyde for 30 min at 4˚C and a flow cytometer was used to count cell number and analyzed by equipped software (CytExpert1.1, Beckman Coulter, Inc., Brea, CA, USA).

Isolation and subculture of BMMSCs. After 2 months maintenance in a SPF room, mice in the OVX and sham groups were anaesthetized, decapitated and immersed in 75% alcohol at 4˚C for 3 min. Mice were subsequently placed in a sterile glass dish, anterior and posterior limbs were separated, and surgery was performed to obtain the marrow cavity of the backbone. This was repeatedly washed in α-MEM until the color of the backbone became pale; the collected cell suspension contained the BMMSCs.

The obtained BMMSCs were seeded in 10-cm plastic petri dishes, containing α-MEM, 20% fetal bovine serum (FBS; Sijiqing Bioengineering Materials Co., Ltd, Hangzhou, China), 1% streptomycin and penicillin, cultured in an atmosphere of 37˚C and 5% CO_2. After 9 days, when BMMSCs had reached 70-80% confluence, cells were treated with 0.25% trypsin and subcultured at a ratio of 1:2. In the following passages, cell medium was refreshed every 2-3 days. When cells reached a confluence of 70-80%, cells were again treated with 0.25% trypsin and subcultured at a ratio of 1:2 or 1:3.

Determination of the immunophenotype of BMMSCs. The obtained third generation BMMSCs were dispersed in 200 μl PBS solution in an Eppendorf (EP) tube with a final concentration of $1x10^5$ cells per EP tube. Then, fluorescein isothiocyanate labeled anti-mouseSca-1 and CD29, and PE-labeled anti-mouseCD45 were added to the BMMSCs cell suspension and incubated in the dark at 4˚C for 1 h. Subsequently, BMMSCs were washed 3 times with PBS solution containing FBS with a concentration of 30 ml/l, centrifuged at 400 x g for 5 min at 4˚C Finally, the fluorescence-labeled BMMSCs were analyzed by flow cytometry. The positive rates of the cell surface antigen of BMMSCs were then analyzed and determined using the built-in software with the unit of %. (CytExpert 1.0.135.2, Beckman Coulter, Inc.).

Differentiation induction of BMMSCs. The obtained third generation BMMSCs were seeded in a 6-well plate with a concentration of $1x10^5$ cells/well. For the induction of differentiation, BMMSCs were either cultured in α-MEM with the addition of 20% FBS, 100 U/ml penicillin, 100 U/ml streptomycin or in osteoblast inducing conditional medium with 10 mM sodium glycerophosphate, 8M dexamethasone and 50 mg/ml vitamin C.

Alkaline phosphatase staining. After 7 days of differentiation induction, the cell medium was removed and the cells were washed 3 times with PBS. Then 4% paraformaldehyde solution was added to fix the cells for 20 min, followed by adding ALP staining solution (33 μl BCIP, 66 μl NBT and 10 ml PBS) and incubated in the dark for 30 min to 24 h. Following two washes with PBS, BMMSCs were imaged by phase-contrast microscopy. Note that the above protocols were strictly followed the instructions of the BCIP/NBT Alkaline Phosphatase Color Development kit (Beyotime Institute of Biotechnology,).

Calcified nodules staining. Following osteogenic induction for 21 days, BMMSCs were washed 3 times with PBS, fixed with 4% paraformaldehyde solution for 1 h, were washed twice again with PBS and finally stained with alizarin red for 15 min at room temperature. After complete removal of the excess alizarin red by three repeated washes with PBS, BMMSCs were imaged via phase-contrast microscopy (magnification, x400).

Adipogenic differentiation induction of BMMSCs. The third generation BMMSCs were seeded in a 6-well plate at a concentration of $1x10^5$ cells/well and incubated with α-MEM supplemented with 20%FBS 100 U/ml penicillin, 100 U/ml streptomycin, 8.9445 g indometacin, 27.8 g IBMX, 500 μl insulin (50 g/l) and 250 μlDex (39.1 g/l) for 14 days in 37˚C. The cell culture medium was replaced every 2 days.

Oil red O staining. After 14 days following adipogenic differentiation, the cell medium was removed and cells were washed three times with PBS. Then, Oil Red O staining solution (0.5 g Oil Red O powder dissolved in 100 ml isopropanol) was added and incubated in the dark for 15 min. After removing the excess oil red O stain, cells were redispersed in PBS and imaged by the phase-contrast microscopy.

Co-culture of BMMSCs with CD4+T lymphocytes. The primary CD4+T lymphocytes derived from normal mice (lymphocytes derived from normal mice for co-culture with sham, OVX and estrogen-treated BMMSCs to observe the pro-apoptotic effect among the BMMSCs from three groups) were seeded in 24-well plates containing equal volume of α-MEM and RPMI-1640 medium at a final concentration of $1x10^6$ cells/well in 37˚C. Normal mice are the mice without sham or OVX operation, which are additional mice to the 40 stated above; the 40 mice stated above were used for osteoporosis or sham models. A total of 20 normal mice (8-weeks-old, 22-25 g, female) were obtained from the Laboratory Animal Center of the Fourth Military Medical University and housed under the same conditions as aforementioned. BMMSCs from each group (OVX, sham and estrogen-treated) were seeded at a concentration of $1x10^4$ cells/well and co-cultured with CD4+T lymphocytes in the same plate for 3 days. For estrogen treatment, the obtained third generation BMMSCs were washed twice with PBS and cultured in 10% FBS containing α-MEM without phenol red. When BMMSCs reached a confluence of 70-80%, estrogen with concentrations of 0, 0.1, 1, 10 and 100 nM were added to the cell medium for 24 h for activation. The activated BMMSCs were kept for further use. Estrogen solutions of various concentrations were prepared by diluting β-estradiol with 50 µl anhydrous ethanol.

Detection of CD4+T lymphocyte apoptosis. CD4+T lymphocyte apoptosis was detected using the Annexin V, 7-aminoactinomycin D (7AAD) and anti-mouse CD4 staining method. Briefly, after 3 days of BMMSCs and CD4+T lymphocyte co-culture, supernatants were collected and centrifuged for 5 min at 400 x g (4˚C). The resultant cell pellets were collected, washed and dispersed in PBS solution containing 3% FBS to a concentration of $1x10^6$ cells/ml. Subsequently, fluorescent anti-mouse CD4 antibody (1:50; BioLegend, Inc., cat. no. 100413) was added and incubated at 4˚C in the dark for 1 h. AnnexinV (5 µl) and 7AAD (5 µl) were subsequently added and the whole system was incubated in the dark at room temperature for 15 min. Finally, the apoptotic ratio of CD4+T lymphocytes was determined by flow cytometry and analyzed by equipped software (CytExpert1.1, Beckman Coulter, Inc.).

Western blot analysis of FasL expression in BMMSCs. BMMSCs from each group (OVX, sham and estrogen-activated BMMSC groups) were washed with 2-3 ml PBS at 4˚C by gentle mixing for 1-2 min. The washing steps were repeated three times and the supernatant was subsequently removed. Washed BMMSCs were placed in an ice-bath, whereas attached BMMSCs were gently scraped and redispersed in PBS at 4˚C and centrifuged for 5 min at 400 x g. Cell pellets were subsequently treated with 1X cell lysis buffer (Beyotime Institute of Biotechnology) according to the instructions provided within the Nuclear and Cytoplasmic Protein Extraction kit (Beyotime Institute of Biotechnology). Suspensions were centrifuged for 12,000 x g with a duration of 5 min at 4˚C and the supernatant was collected for western blot analysis. Proteins were quantified with a Bicinchoninic Acid protein assay. Equal amounts (40 µg) of proteins were loaded on 10% SDS-PAGE. Following separation, proteins were transferred to polyvinylidene fluoride membranes (EMD Millipore, Billerica, MA, USA). The membranes were blocked with 5% bovine serum albumin (BSA) blocking buffer (Sigma-Aldrich, Merck KGaA) and then were incubated overnight at 4˚C with the primary antibodies (FasL and β-actin, 1:50 dilution). The membranes were then incubated with goat anti-rabbit IgG (H+L) secondary antibody (unconjugated) (Wuhan Boster Biological Biological Technology, Ltd., Wuhan, China) at room temperature for 2 h. The blots on the membranes were analyzed using imaging system (WD-9423C, Beijing Liuyi Biotechnology, Co., Ltd., Beijing, China) under treatment of an enhanced chemiluminescence kit (GE Healthcare, Chicago, IL, USA).

Microarray. Total RNAs were isolated from BMMSCs of Sham and OVX mice, and were analyzed using microRNA microarray (uParaflo platform, Sanger 17.0, LC Science Inc. Shanghai, China). Raw data were normalized by Quantile algorithm (22). Prediction of target genes was analyzed using the online database miRbase, release 22.0 (www.mirbase.org).

Reverse transcription-quantitative polymerase chain reaction (RT-qPCR). Total RNA was extracted from OVX, Sham and estrogen-treated BMMSCs. Total RNA was isolated using TRIzol reagent according to the manufacturer's protocols. miR-181aprimers were designed and synthesized by Guangzhou RiboBio Co., Ltd. (Guangzhou, China); sequences are listed in Table I. The PCR reaction mixture included: SYBR® Green Mix (10 µl), RT template (2 µl), Bulge-Loop™ miRNA forward (1 µl; 5 µM), Bulge-Loop™ miRNA reverse (1 µl; 5 µM) and RNase-free H_2O (5 µl). The thermocycling conditions were as follows: Initial denaturation at 95˚C for 3 min, followed by 40 cycles of denaturation at 95˚C for 30 sec, annealing for 30 sec and extension at 72˚C for 30 sec. The fluorescent signals were recorded during the extension process and the data were analyzed using the dissolution curve (95˚C for 15 sec, 60˚C for 23 sec and 95˚C for 15 sec) at the end of all cycles. The data were normalized using $2^{-\Delta\Delta Cq}$ (23).

RNA extraction. A total of 1 ml TRIzol was added to each well; $2x10^6$ cells were incubated for 6 min. The lysis solution was then transferred to 1.5 ml EP tube with the addition of 0.2 ml chloroform. The tube was shaken vigorously for 15 min and incubated at 15-30˚C for 2-3 min, followed by centrifugation at 10,000 x g for 15 min at 4˚C. After careful removal of the upper layer into a new EP tube, an equal volume of isopropanol was added, and the EP tube was placed in the -20˚C fridge without disturbance for 1 h, then centrifuged at 10,000 x g for 15 min at 4˚C. After removing the supernatant, 500 µl 75% ethanol was added to disperse the precipitates and gently mixed for 30 sec, followed by centrifugation at 10,000 x g for 5 min at 4˚C. The resultant supernatant was removed and the precipitates in the tube were dried under RNase free condition for 3-5 min. Finally, 20 µl DEPC was added to dissolve the dried precipitates and the RNA solution was saved in a fridge under -80˚C.

RNA detection. A total of 2 µl of the aforementioned obtained RNA solution with 1 µl buffer and then 1.5% agarose gel electrophoresis was used for RNA detection at a voltage of 80 V. After 30 min run in a fresh 1X TBE buffer, band 185 and 285 representing RNA sample in the gel were detected by

Table I. Oligonucleotide primers used for polymerase chain reaction.

Primer	Sequence	Product size (bp)	Tm
MicroRNA-181a	F: 5'-AACATTCAACGCTGTCGGTGAGT-3' R: 5'-CTCCTTAGAATCTGTTTGCTCTCATA-3'	118	62˚C
U6	F: 5'-CTCGCTTCGGCAGCACA-3' R: 5'-AACGCTTCACGAATTTGCGT-3'	88	60.6˚C

bp, base pairs; F, forward; R, reverse; Tm, primer melting temperature.

UV transmission detector. Finally, the RNA concentration was determined using an EP RNA detector.

RNA reverse transcription. The reaction solution was prepared according to the instructions of Bulge-loop™ miRNA-qRT-PCR Primer containing 10 μl 2X miRNA Reaction Buffer Mix (RT), 2 μl 0.1%BSA, 2 μl miRNA PrimeScriptRT Enzyme Mix, 1 μl total RNA, and 5 μl RNase Free ddH_2O. The prepared reaction solution was placed in the PCR amplifier for RT: 42˚C, 60 min and 70˚C, 10 min for 40 cycles. Subsequently, cDNA derived from sham, OVX and estrogen-treated BMMSCs was collected and placed on ice for microRNA detection.

miR-181a cell transfection. A total of 1 day prior to transfection, the appropriate number of BMMSCs was seeded into the wells of a culture plate, and cells were cultured in α-MEM without antibiotics until cell confluence reached 30-50%. Cell density is a key factor that affects transfection efficiency, and cell overgrowth weakens their activity and reduces transfection efficiency. miRNA mimic (miR10000858-1-5), inhibitor (miR20000858-1-5), control (miR30017138-1-10) (1.25 μl) and Lipofectamine® 2000 were separately diluted with 50 μl serum-free α-MEM, mixed gently and incubated at room temperature for 5 min for further use. The diluted solutions were mixed gently and incubated at room temperature for 20 min. The prepared transfection solution was added to the bottom of each well of the 12-well plate and $5x10^4$ cells/well were added. The cells were incubated at 37˚C for 24 h. miR-181a mimic, inhibitor or control-transfected BMMSCs were also used for intravascular injection at a dose of $5x10^5$ cells. After 5 days following the administration of transfected BMMSCs, the *in vivo* lymphocytes were collected and used for apoptosis analysis by flow cytometry as aforementioned.

Statistical analysis. Statistical analysis was performed using SPSS11.0 software (SPSS, Inc., Chicago, IL, USA). Comparison of multiple groups was performed using one way analysis of variance followed by a Tukey's post-hoc test. The means of two independent samples were compared using Student's t-test. $P<0.05$ was considered to indicate a statistically significant difference.

Results

Isolation and identification of BMMSCs. A mouse model of osteoporosis was established and verified by Micro-CT analysis (Table II). BMMSCs were subsequently isolated from the mice in the OVX and sham groups, and their immunophenotype and multi-potent differentiation abilities were examined. The obtained BMMSCs were revealed to possess stem cell-like characteristics and multi-potent differentiation ability (data not shown).

Comparison of CD4$^+$T lymphocyte numbers in each group. A previous study indicated that estrogen deficiency activates T lymphocytes and disrupts the dynamic balance between bone resorption and formation (8). Therefore, in the present study, CD4$^+$T cells were isolated from mice in the sham (Fig. 1A and B) and OVX groups (Fig. 1C and D), and cell numbers were determined by flow cytometry. As shown in Fig. 1E, the percentage of CD_4^+T lymphocytes was determined in total spleen cells. The number of CD4$^+$T lymphocytes in the OVX group was markedly higher compared within the Sham group, thus suggesting that estrogen deficiency may increase the number of CD4$^+$T lymphocytes.

Apoptotic effects of estrogen-treated BMMSCs on CD4$^+$ T lymphocytes. Our previous work demonstrated that BMMSCs induce osteoclast apoptosis and estrogen promotes BMMSCs-induced osteoclast apoptosis (18). In the present study, the apoptotic effects of BMMSCs on CD4$^+$T lymphocytes were examined. Isolated BMMSCs from the OVX group were activated by treatment with estrogen at various concentrations. Estrogen-treated BMMSCs were co-cultured with CD4$^+$T lymphocytes for 3 days (OVX+ estrogen group) and CD4$^+$T lymphocyte apoptosis in the co-culture system was subsequently determined. As a control, CD4$^+$T lymphocytes were co-cultured with untreated BMMSCs from the OVX and sham groups, and the apoptotic rate was determined. Annexin V was used to label early apoptotic and necrotic cells, 7AAD was used to label late apoptotic and necrotic cells, and anti-mouse CD4 antibody was used to specifically investigate CD4$^+$T lymphocytes. The flow cytometry results of the OVX (Fig. 2A), sham (Fig. 2B) and OVX+E2 groups (Fig. 2C) revealed that the apoptotic rate of CD4$^+$T lymphocytes in the OVX+E2 group was markedly higher, compared with that in the sham or OVX groups. The apoptotic rate of CD4$^+$T lymphocytes in the OVX group was the lowest among the three groups (Fig. 2D). These results suggested that BMMSCs may have an apoptotic effect on CD4$^+$T lymphocytes and that estrogen significantly increased this effect.

Table II. Microtomography results of the sham and OVX groups.

Group	BV/TV (%)	BS/BV (1/mm)	Tb.Th (mm)	Tb.N (1/mm)	Tb.Sp (mm)	BMD (mg/cc)
Sham	21.15±3.42	25.34±3.12	0.840±0.08	2.01± 0.4	0.41±0.11	408.80±21.55
OVX	5.32±1.65[a]	8.98±4.05[b]	0.051±0.02[a]	.42±0.6[b]	0.82±0.16[b]	60.45±18.79

[a]P<0.01, [b]P<0.05 vs. the sham group. BMD, bone mineral density; BS/BV, bone surface relative to bone volume; BV/TV, bone volume relative to tissue volume; OVX, bilateral ovariectomy group; Tb.N, trabecular bone number; Tb.Sp, trabecular bone spacing; Tb.Th, trabecular bone thickness.

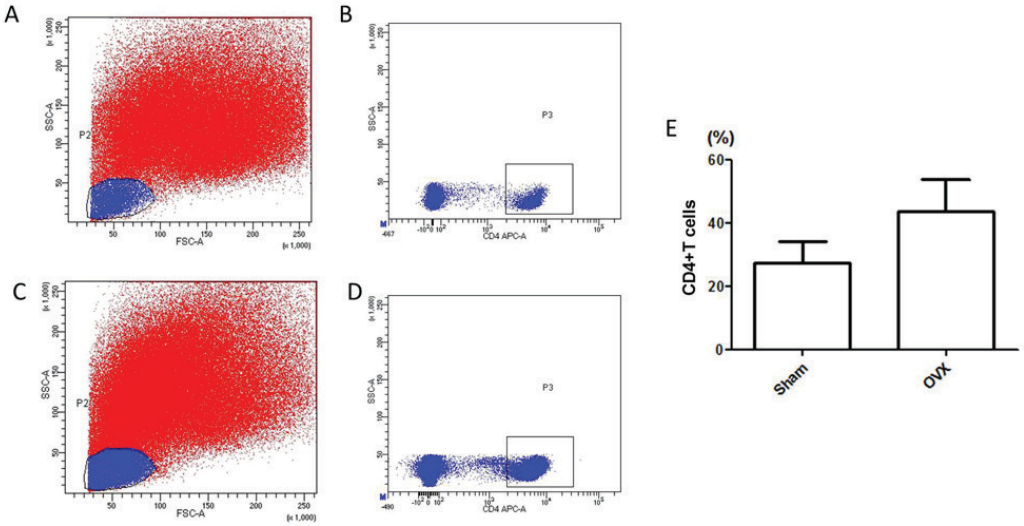

Figure 1. Flow cytometry was used to detect CD4+ T lymphocytes in the (A and B) sham and (C and D) OVX groups; cell debris was excluded. (E) The percentage of CD4+ T cells were increased within OVX mice compared to Sham mice. CD4, cluster of differentiation 4; OVX, bilateral ovariectomy group.

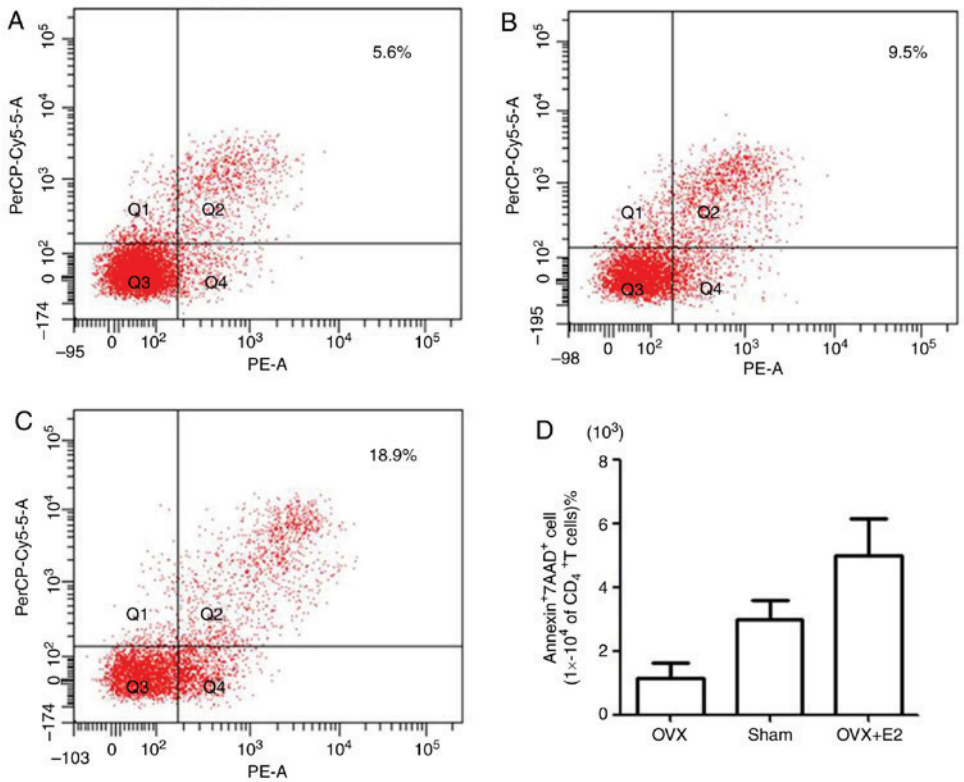

Figure 2. Flow cytometric analysis of CD4+T lymphocyte apoptosis in the (A) OVX, (B) sham and (C) OVX+E2groups. (D) Comparison of the apoptotic rates of CD4+T lymphocytes in each group. 7AAD, 7-aminoactinomycin D; CD4, cluster of differentiation 4; E2, estrogen; OVX, bilateral ovariectomy group.

Regulatory effects of estrogen on FasL expression in BMMSCs. BMMSCs have been reported to induce T-cell apoptosis via FasL expression (24). To investigate the regulatory effects of estrogen on the protein expression levels of FasL in BMMSCs, western blot analysis was performed in the three co-culture systems. The results revealed that FasL protein expression was markedly lower in BMMSCs from the OVX group compared with in the sham group (Fig. 3A). Gradually increasing concentrations of estrogen resulted in a marked increase in FasL expression (Fig. 3B), whereas >10 mM estrogen may not further increase the expression of FasL. These findings indicated that estrogen may promote CD4$^+$T lymphocyte apoptosis by increasing FasL protein expression in BMMSCs.

miR-181a expression in BMMSCs. It has previously been reported that miRNAs are important in the regulation of BMMSC function. According to a previous study it was demonstrated that miRNA-21 expression is decreased in BMMSCs following surgical ovariectomy (25). In addition, it has been demonstrated that miR-181a expression is significantly increased in an OVX group (18). In the present study, the expression levels of miR-181a in the three different co-culture systems were determined by RT-qPCR. miR-181a expression was significantly higher in the OVX group compared with in the sham group (Fig. 4A). Conversely, estrogen treatment decreased miR-181a expression in BMMSCs in a concentration-dependent manner; however, when estrogen concentration reached 100 nM, miR-181a expression was increased to some extent compared with the levels detected following treatment with 10 nM estrogen, thus indicating that excessive estrogen may exert an inverse effect (Fig. 4B).

Effects of miR-181a transfection on FasL expression in BMMSCs. miR-181a was transfected into BMMSCs to determine the regulatory effects of miR-181a on FasL protein expression in BMMSCs. BMMSCs were transfected with miR-181a mimic, miR-181a inhibitor, mimic control or inhibitor control. The transfection efficiency of the miR-181a mimic and the miR-181a inhibitor was confirmed by RT-qPCR. Compared with in the mimic control group, the expression levels of miR-181a were increased by ~50-fold in BMMSCs transfected with the miR-181a mimic (Fig. 4C), whereas miR-181a expression was ~15 times lower in BMMSCs transfected with the miR-181a inhibitor compared with the inhibitor control (Fig. 4D). These data suggested that the miR-181a mimic and miR-181a inhibitor were transfected into BMMSCs with high efficiency.

Western blot analysis was subsequently performed to detect FasL protein levels in each group. FasL protein expression in BMMSCs transfected with the miR-181a mimic was markedly inhibited compared with in the mimic control group, whereas a significant increase in FasL protein expression was detected in BMMSCs transfected with the miR-181a inhibitor compared with the inhibitor control (Fig. 4E).

In vitro regulatory effect of miR-181a on CD4$^+$T lymphocyte apoptosis. Our previous work revealed a negative regulatory effect of miR-181a on BMMSCs-induced osteoclast apoptosis (18). Therefore, the regulatory effects of miR-181a on BMMSC-induced CD4$^+$T lymphocyte apoptosis were examined in the present study. BMMSCs were transfected with miR-181a mimic, mimic control and miR-181a inhibitor. The transfected BMMSCs were subsequently co-cultured with CD4$^+$T lymphocytes, in order to determine their apoptotic effect on CD4$^+$T lymphocytes. Flow cytometric analysis revealed that miR-181a mimic transfection resulted in a significant reduction in the proportion of apoptotic cells (5.1%; Fig. 5A) compared with the control group (11.0%; Fig. 5B); however, miR-181a inhibitor transfection resulted in an increased number of apoptotic cells (24.0%; Fig. 5C), thus indicating the regulatory effect of miR-181a on BMMSC-induced CD4$^+$T lymphocyte apoptosis (Fig. 5D).

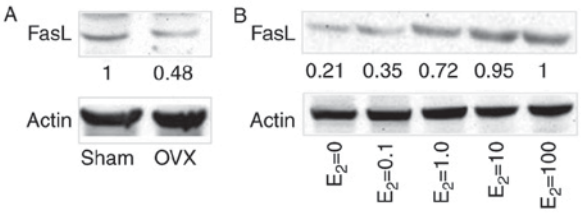

Figure 3. Western blot analysis of FasL expression in BMMSCs in the (A) OVX and sham groups. (B) FasL protein expression in the OVX group BMMSCs in response to increasing estrogen concentrations. BMMSCs, bone marrow mesenchymal stem cells; OVX, bilateral ovariectomy group; FasL, Fas ligand.

In vivo regulatory effect of miR-181a on CD4$^+$ T lymphocyte apoptosis. To validate the *in vivo* regulatory effects of miR-181a on CD4$^+$T lymphocyte apoptosis, BMMSCs transfected with miR-181a mimic, mimic control and miR-181a inhibitor were intravenously injected into mice. After 7 days of treatment, alterations in mouse bone content were determined by micro-CT. The bone volume of mice treated with the miR-181a mimic (Fig. 6A) was markedly lower compared with in the control group (Fig. 6B). Conversely, mice in the miR-181a inhibitor group (Fig. 6C) had a visibly higher bone volume than the control group. The derivate parameters from the micro-CT measurements (Table III) further confirm these findings; bone mass measurements, including BV/TV, BS/BV and BMD, were significantly decreased in the miR-181a mimic-treated group compared with in the control group. Conversely, the opposite effect was observed in the group treated with the miR-181a inhibitor.

Furthermore, alterations in the apoptotic rate of CD4$^+$T lymphocytes were detected after 2 days of injection with BMMSCs transfected with miR-181a mimic, mimic control and miR-181a inhibitor. The apoptotic rate of CD_4^+T lymphocytes in mice treated with the miR-181a mimic (Fig. 4D) was markedly decreased compared with in the control group (Fig. 4E), whereas apoptosis was markedly increased in the miR-181a inhibitor-treated group (Fig. 6F), which further demonstrated the effects of miR-181a on CD4$^+$ T lymphocyte apoptosis (Fig. 6G).

Discussion

It has previously been reported that PMO is a bone formation disorder caused by estrogen deficiency (14). Estrogen

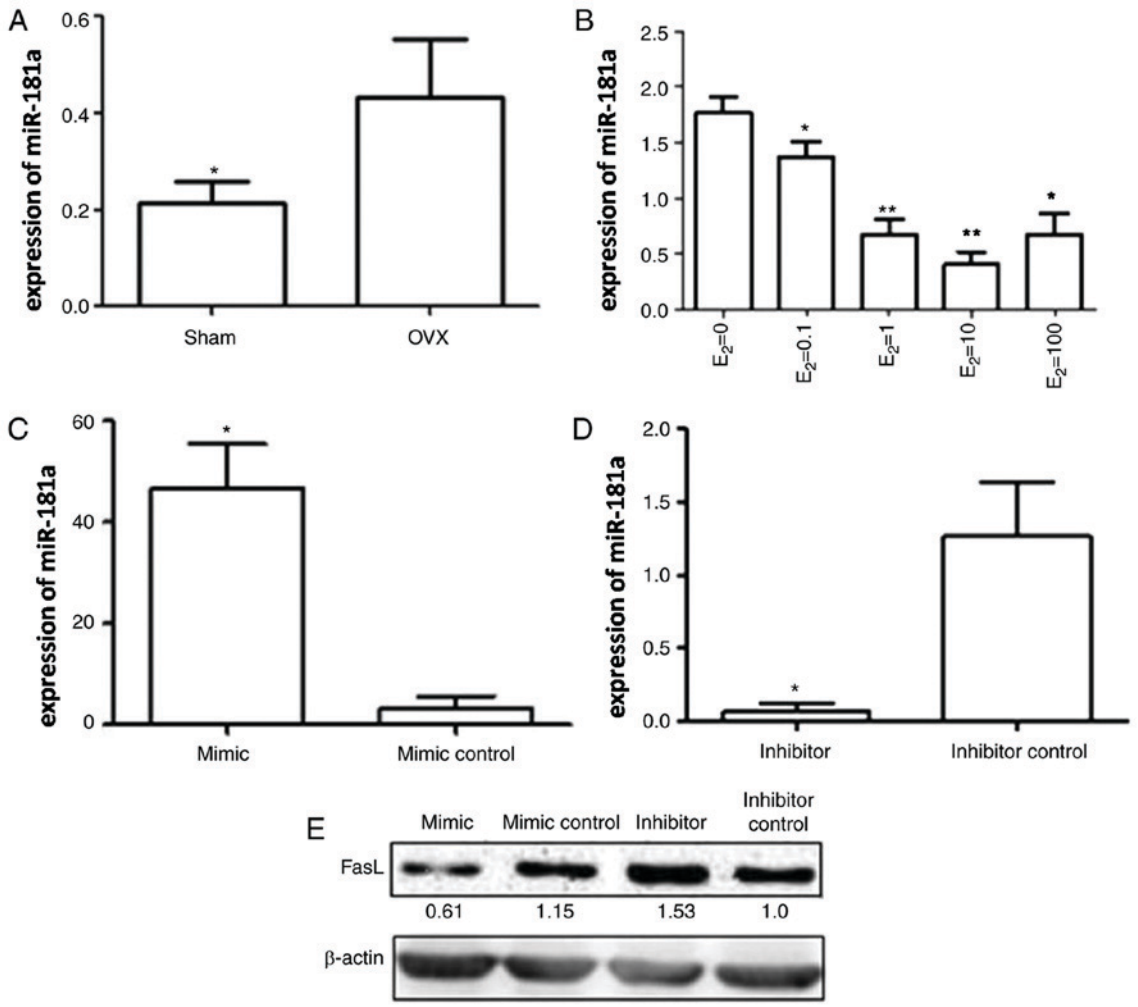

Figure 4. Effects of miR-181a expression on FasL protein expression in BMMSCs. (A) miR-181a expression levels in the OVX and sham groups. (B) Increasing concentrations of estrogen were added to BMMSCs and miR-181a expression levels were detected. (C) miRNA-181a mimic (D) and miRNA-181a inhibitor transfection efficiency was determined. (E) Alterations in the protein expression levels of FasL in BMMSCs transfected with miR-181a mimic, miR-181a inhibitor, mimic control and inhibitor control were determined by western blot analysis. BMMSCs, bone marrow mesenchymal stem cells; FasL, Fas ligand; miR-181a, microRNA-181a; OVX, bilateral ovariectomy group. *P<0.05 vs. 0 nM, mimic or inhibitor controls. **P<0.01 vs. 0 nM.

deficiency facilitates the differentiation and maturation of osteoclasts by inducing the expression of RankL/Rank in T lymphocytes (26). The results of the present study demonstrated that estrogen affected BMMSC-induced apoptosis of CD_4^+T lymphocytes. The present study also suggested that the regulatory effects of estrogen on BMMSC-induced CD4$^+$ T lymphocyte apoptosis may be mediated by FasL protein expression in BMMSCs, with estrogen increasing FasL protein expression. However, no difference in FasL protein expression was detected in BMMSCs when estrogen concentration reached 100 nM compared with 10 nM treatment. This may be due to the presence of an estrogen response element (ERE) on the promoter sequence of the FasL gene, which integrates with the estrogen-activated estrogen receptor (ER) to promote gene expression of FasL (27); when estrogen concentration is too high, the integration ability between ERE and ER may be weakened, thus reducing the regulatory effect of estrogen on FasL expression (28).

Estrogen has been reported to affect miRNA expression in zebrafish, mice and ACI rats (29,30). It has been revealed that estrogen inhibits osteoblast apoptosis through upregulation of miR-17-92a (31). In addition, estrogen treatment results in the increased expression of miR-146a, miR-125a, miR-125b, let-7e and miR-126 in T lymphocytes isolated from mouse spleen (32). Previous studies have suggested that miR-181a is involved in cell differentiation and development, as well as immunological, cardiovascular and central nervous system diseases (33-35). In the present study, miRNAs that upregulate BMMSCs in mice with osteoporosis were selected using genechips, and miR-181a was selected as the miRNA of interest based on miRNA target gene prediction software.

The present study observed that miR-181a expression in BMMSCs was markedly increased in the OVX group, which may be due to the decrease in estrogen during the development of osteoporosis following ovary removal. Conversely, the expression levels of miR-181a were significantly reduced in BMMSCs treated with estrogen at a concentration of 0.1, 1 and 10 nM, thus demonstrating the negative regulatory effect of estrogen on miR-181a expression within a certain concentration range. In addition, a significant decrease in CD4$^+$T lymphocyte apoptosis was observed following the

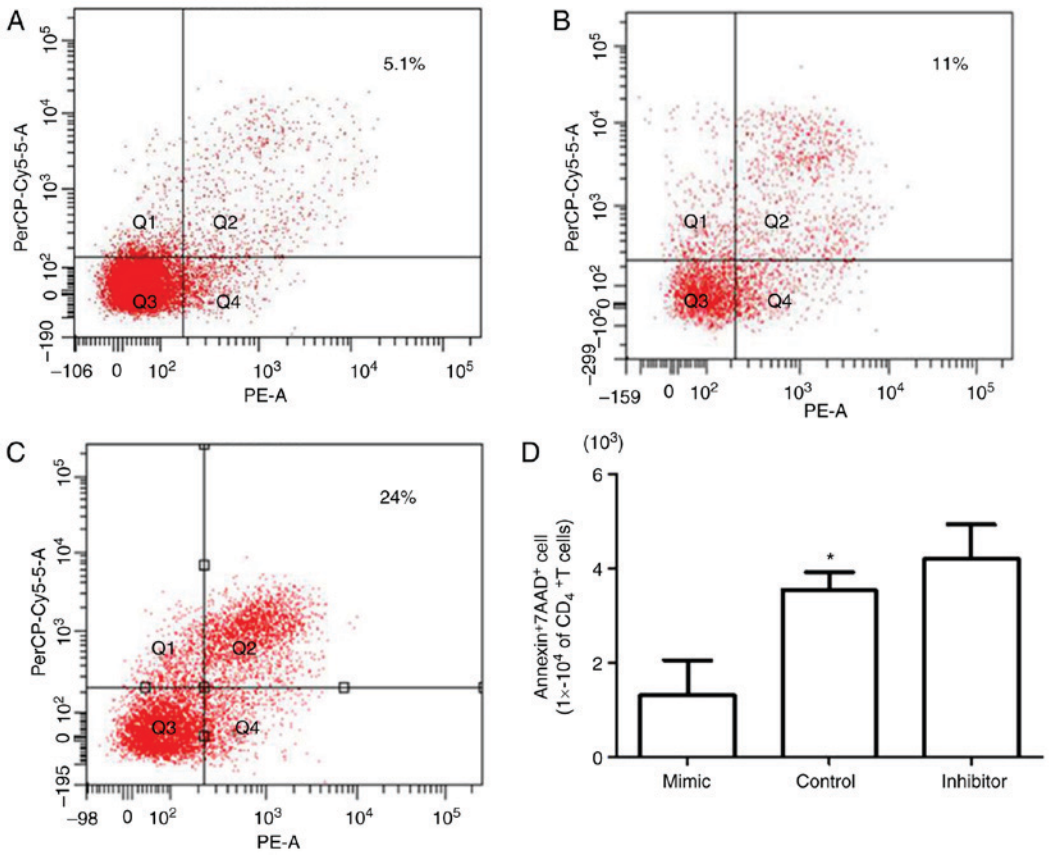

Figure 5. Flow cytometric analysis of the apoptotic rate of $CD4^+$ T cells co-cultured with BMMSCs transfected with (A) miR-181a mimic, (B) mimic control or (C) miR-181a inhibitor. (D) Comparison of the apoptotic rate of $CD4^+$T lymphocytes in each group. 7AAD, 7-aminoactinomycin D; BMMSCs, bone marrow mesenchymal stem cells; CD4, cluster of differentiation 4; miR-181a, microRNA-181a. *P<0.05 vs. mimic.

upregulation of miR-181a expression; this may be due to the inhibited expression of $CD4^+$ T lymphocyte apoptosis-associated factors in BMMSCs, including FasL. By performing western blot analyses, it was revealed that the expression levels of the apoptotic protein, FasL, were reduced in BMMSCs following miR-181amimic transfection. In conclusion, it may be suggested that miR-181 affects BMMSCs-mediated apoptosis of $CD4^+$T lymphocytes via the regulation of FasL protein expression; this regulatory ability may be directly associated with estrogen concentration. A previous study reported similar results, that estrogen induces the expression of B-cell lymphoma 2, cyclin D1 and survivin by inhibiting the expression of miR-6, miR-143 and miR-203 in MCF-7 cells. In addition, the regulatory effects of estrogen are eliminated by estrogen inhibitors (36). In addition, further study may be conducted to investigate the downstream signaling underlying miR-181a/FasL to understand mechanism of osteoporosis and to develop a novel therapy for osteoporosis, by potentially targeting the regulation of miR-181a.

Acknowledgements

The authors would like to thank the Chongqing Municipal Key Laboratory of Oral Biomedical Engineering of Higher Education and the Program from Innovation Team Building at Institutions of Higher Education of Chongqing, 2016 for support of basic medicine research. The authors would also thank to Miss Hua Ni for molecular and cellular experiments assistance, and thank Mr. Xiaolin Xu for assisting with the animal experiments (Research and Development Center for Tissue Engineering, Fourth Military Medical University (Xi'an, China).

Funding

This research was funded by the General Program of National Natural Science Foundation of China (grant no. 31571508) and the General Program of National Natural Science Foundation of China (grant no. 31371473).

Availability of data and materials

All data generated or analyzed during this study are included in this published article.

Author's contributions

BS made substantial contributions to the conception and design, collection and assembly of data, data analysis and interpretation, wrote the manuscript. XF made substantial contributions to the design of the present study, collection, analysis and interpretation of data; YY made contributions in modifying the study design, assembly of data and data analysis and interpretation. DY made substantial contributions to the conception and design of the present study, data analysis and interpretation, wrote the manuscript and gave final approval

Table III. Microtomography results of the mice treated with microRNA-181a mimic, inhibitor or control for 7 days.

Group	BV/TV (%)	BS/BV (1/mm)	Tb.Th (mm)	Tb.N (1/mm)	Tb.Sp (mm)	BMD (mg/cc)
Mimic	5.15±3.02	25.34±3.12	0.040±0.08	2.01±0.4	0.91±0.11	150.80±21.55
Control	10.32±1.65[a]	30.98±4.05[b]	0.51± 0.02[a]	4.42±0.6[b]	0.71±0.16[b]	250.45±16.09[b]
Inhibitor	19.45±3.42	28.31±3.10	0.840±0.08	2.01± 0.4	0.41±0.11	370.80±21.55

[a]P<0.01 (compared to mimic), [b]P<0.05 (compared to mimic) BMD, bone mineral density; BS/BV, bone surface relative to bone volume; BV/TV, bone volume relative to tissue volume; Tb.N, trabecula number; Tb.Sp, trabecular spacing; Tb.Th, trabecula thickness.

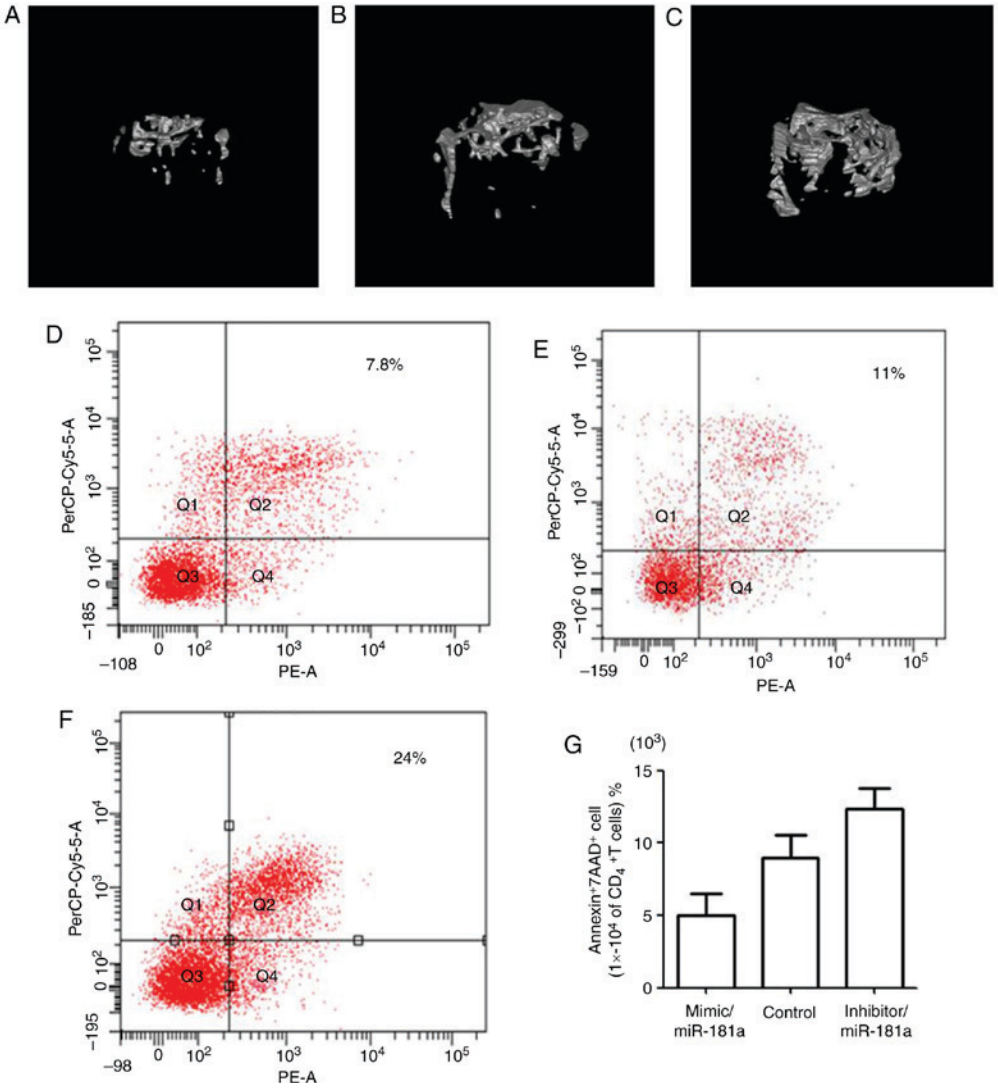

Figure 6. Representative microtomography images of mouse bone and analysis of CD4⁺ T lymphocyte apoptosis. Mice were treated with BMMSCs transfected with (A) miR-181a mimic, (B) mimic control or (C) miR-181a inhibitor. Flow cytometric analysis of apoptosis of CD4⁺T lymphocytes from mice treated with (D) miR-181a mimic, (E) mimic control or (F) miR-181a inhibitor. (G) Comparison of the apoptotic rate of CD4⁺T lymphocytes in each group. 7AAD, 7-aminoactinomycin D; BMMSCs, bone marrow mesenchymal stem cells; CD4, cluster of differentiation 4; miR-181a, microRNA-181a.

of version to be published. All authors read and approved the manuscript.

Ethics approval and consent to participate

The present study was approved by the ethics committee of Chongqing Medical University (Chongqing, China).

Consent for publication

Not applicable.

Competing interests

The authors declare that they have no competing interests.

References

1. Rachner TD, Khosla S and Hofbauer LC: Osteoporosis: Now and the future. Lancet 377: 1276-1287, 2011.
2. Weitzmann MN and Pacifici R: Estrogen deficiency and bone loss: An inflammatory tale. J Clin Invest 116: 1186-1194, 2006.
3. Roggia C, Gao Y, Cenci S, Weitzmann MN, Toraldo G, Isaia G and Pacifici R: Up-regulation of TNF-producing T cells in the bone marrow: A key mechanism by which estrogen deficiency induces bone loss in vivo. Proc Natl Acad Sci USA 98: 13960-13965, 2001.
4. Duque G, Huang DC, Dion N, Macoritto M, Rivas D, Li W, Yang XF, Li J, Lian J, Marino FT, *et al*: Interferon-γ plays a role in bone formation in vivo and rescues osteoporosis in ovariectomized mice. J Bone Min Res 26: 1472-1483, 2011.
5. Cenci S, Toraldo G, Weitzmann MN, Roggia C, Gao Y, Qian WP, Sierra O and Pacifici R: Estrogen deficiency induces bone loss by increasing T cell proliferation and lifespan through IFN-gamma-induced class II transactivator. Proc Natl Acad Sci USA 100: 10405-10410, 2003.
6. Kudo O, Sabokbar A, Pocock A, Itonaga I, Fujikawa Y and Athanasou NA: Interleukin-6 and interleukin-11 support human osteoclast formation by a RANKL-independent mechanism. Bone 32: 1-7, 2003.
7. Hartgring SAY, Bijlsma JWJ, Lafeber FPJG and van Roon JAG: Interleukin-7 induced immunopathology in arthritis. Ann Rheumatic Dis 65: iii69-iii74, 2006.
8. Han X, Kawai T, Eastcott JW and Taubman MA: Bacterial-Responsive B Lymphocytes Induce Periodontal Bone Resorption. J Immunol 176: 625-631, 2006.
9. Zhu J and Paul WE: CD4 T cells: Fates, functions, and faults. Blood 112: 1557-1569, 2008.
10. Kikuta J, Wada Y, Kowada T, Wang Z, Sun-Wada GH, Nishiyama I, Mizukami S, Maiya N, Yasuda H, Kumanogoh A, *et al*: Dynamic visualization of RANKL and Th17-mediated osteoclast function. J Clin Invest 123: 866-873, 2003.
11. Griffith TS, Brunner T, Fletcher SM, Green DR and Ferguson TA: Fas ligand-induced apoptosis as a mechanism of immune privilege. Science 270: 1189-1192, 1995.
12. Siegel RM, Frederiksen JK, Zacharias DA, Chan FK, Johnson M, Lynch D, Tsien RY and Lenardo MJ: Fas preassociation required for apoptosis signaling and dominant inhibition by pathogenic mutations. Science 288: 2354-2357, 2000.
13. Nakamura T, Imai Y, Matsumoto T, Sato S, Takeuchi K, Igarashi K, Harada Y, Azuma Y, Krust A, Yamamoto Y, *et al*: Estrogen prevents bone loss via estrogen receptor alpha and induction of fas ligand in osteoclasts. Cell 130: 811-823, 2007.
14. Krum SA, Miranda-Carboni GA, Hauschka PV, Carroll JS, Lane TF, Freedman LP and Brown M: Estrogen protects bone by inducing Fas ligand in osteoblasts to regulate osteoclast survival. EMBO J 27: 535-545, 2008.
15. Krampera M, Glennie S, Dyson J, Scott D, Laylor R, Simpson E and Dazzi F: Bone marrow mesenchymal stem cells inhibit the response of naive andmemory antigen-specific T cells to their cognate peptide. Blood 101: 3722-3729, 2003.
16. Rosado MM, Bernardo ME, Scarsella M, Conforti A, Giorda E, Biagini S, Cascioli S, Rossi F, Guzzo I, Vivarelli M, *et al*: Inhibition of B-cell proliferation and antibody production by mesenchymal stromal cells is mediated by T cells. Stem Cells 24: 93-103, 2015.
17. Schurgers E, Kelchtermans H, Mitera T, Geboes L and Matthys P: Discrepancy between the in vitro and in vivoeffects of murine mesenchymal stem cells onT-cell proliferation and collagen-induced arthritis. Arthritis Res Ther 12: R31, 2003.
18. Tang Y, Wu X, Lei W, Pang L, Wan C, Shi Z, Zhao L, Nagy TR, Peng X, Hu J, *et al*: TGF-beta1-induced migration of bone mesenchymal stem cells couples bone resorption with formation. Nat Med 15: 757-765, 2009.
19. Zhao H, Xu H and Xue L: Regulatory network involving miRNAs and genes in serous ovarian carcinoma. Oncol Lett 14: 6259-6268, 2007.
20. Sugatani T and Hruska KA: Down-regulation of miR-21 biogenesis by estrogen action contributes to osteoclastic apoptosis. J Cell Biochem 114: 1217-1222, 2003.
21. Shao B, Liao L, Yu Y, Shuai Y, Su X, Jing H, Yang D and Jin Y: Estrogen preserves Fas ligand levels by inhibiting microRNA-181a in bone marrow-derived mesenchymal stem cells to maintain bone remodeling balance. FASEB J 29: 3935-3944, 2015.
22. Bolstad BM, Irizarry RA, Astrand M and Speed TP: A comparison of normalization methods for high density oligonucleotide array data based on variance and bias. Bioinformatics 19: 185-193, 2003.
23. Livak KJ and Schmittgen TD: Analysis of relative gene expression data using real-time quantitative PCR and the 2(-Delta Delta C(T)) method. Methods 25: 402-408, 2001.
24. Akiyama K, Chen C, Wang D, Xu X, Qu C, Yamaza T, Cai T, Chen W, Sun L and Shi S: Mesenchymal-stem-cell-induced immunoregulation involves FAS-ligand-/FAS-mediated T cell apoptosis. Cell Stem Cell 10: 544-555, 2012.
25. Yang N, Wang G, Hu C, Shi Y, Liao L, Shi S, Cai Y, Cheng S, Wang X and Liu Y, *et al*: Tumor necrosis factor α suppresses the mesenchymal stem cell osteogenesis promoter miR-21 in estrogen deficiency-induced osteoporosis. J Bone Miner Res 28: 559-573, 2003.
26. Hsu H, Lacey DL, Dunstan CR, Solovyev I, Colombero A, Timms E, Tan HL, Elliott G, Kelley MJ, Sarosi I, *et al*: Tumor necrosis factor receptor family member RANK mediates osteoclast differentiation and activation induced by osteoprotegerin ligand. Proc Natl Acad Sci USA 96: 3540-3545, 1999.
27. Mor G, Kohen F, Garcia-Velasco J, Nilsen J, Brown W, Song J and Naftolin F: Regulation of Fas ligand expression in breast cancer cells by estrogen: Functional differences between estradiol and tamoxifen. J Steroid Biochem Mol Biol 73: 185-194, 2003.
28. Cohen A, Shmoish M, Levi L, Cheruti U, Levavi-Sivan B and Lubzens E: Alterations in Micro-ribonucleic acid expression profiles reveal a novel pathway for estrogen regulation. Endocrinology 149: 1687-1696, 2008.
29. Kovalchuk O, Tryndyak VP, Montgomery B, Boyko A, Kutanzi K, Zemp F, Warbritton AR, Latendresse JR, Kovalchuk I, Beland FA and Pogribny IP: Estrogen-induced rat breast carcinogenesis is characterized by alterations in DNA methylation, histone modifications, and aberrant microrna expression. Cell Cycle 6: 2010-2018, 2007.
30. Dai R, Phillips RA, Zhang Y, Khan D, Crasta O and Ahmed SA: Suppression of LPS-induced Interferon-gamma and nitric oxide in splenic lymphocytes by select estrogen-regulated microRNAs: A novel mechanism of immune modulation. Blood 112: 4591-4597, 2008.
31. Guo L, Xu J, Qi J, Zhang L, Wang J, Liang J, Qian N, Zhou H, Wei L and Deng L: MicroRNA-17-92a upregulation by estrogen leads to Bim targeting and inhibition of osteoblast apoptosis. J Cell Sci 126: 978-988, 2003.
32. Naguibneva I, Ameyar-Zazoua M, Polesskaya A, Ait-Si-Ali S, Groisman R, Souidi M, Cuvellier S, and Harel-Bellan A: The microRNA miR-181 targets the homeobox protein Hox-A11 during mammalian myoblast differentiation. Nat Cell Biol 8: 278-284, 2006.
33. Kumar S, Naqvi RA, Khanna N and Rao DN: Disruption of HLA-DR raft, deregulations of Lck-ZAP-70-Cbl-b cross-talk and miR181a towards T cell hyporesponsiveness in leprosy. Mol Immunol 48: 1178-1190, 2011.
34. Li YG, Zhang PP, Jiao KL and Zou YZ: Knckdown of microRNA-181 by lentivirus mediated siRNA expression vector decreases the arrhythmogenic effect of skeletal myoblast transplantation in rat with mycardial infarction. Microvasc Res 78: 393-404, 2009.
35. Ouyang YB, Lu Y, Yue S, Xu LJ, Xiong XX, White RE, Sun X and Giffard RG: miR-181 regulates GRP78 and influences outcome from cerebral ischemia in vitro and in vivo. Neurobiol Dis 45: 555-563, 2012.
36. Yu X, Zhang X, Dhakal IB, Beggs M, Kadlubar S and Luo D: Induction of cell proliferation and survival genes by estradiol-repressed microRNAs in breast cancer cells. BMC Cancer 12: 29, 2012.